American Journal of Pathology, Vol. 142, No. 5, May 1993

Podocytic Cytoskeletal Disaggregation and Basement-Membrane Detachment in Puromycin Aminonucleoside Nephrosis

Catharine I. Whiteside, Richard Cameron, Snezana Munk, and Jacob Levy

From the Medical Research Council of Canada, Group in Membrane Biology, Department of Medicine, University of Toronto, Toronto, Ontario, Canada

Puromycin aminonucleoside– (PAN) treated rats develop acute nephrotic syndrome, mimicking human minimal lesion disease. In PAN nephrosis, podocyte detachment from the glomerular basement membrane (GBM) is the most likely cause of massive proteinuria in this model. To elucidate further the mechanism of PAN-induced cellular dysfunction, new methods were employed to visualize podocyte cytoskeletal aggregation and to measure fibrillar attachment to the GBM. Adult Sprague-Dawley rats (n = 4/group) received a single tail-vein injection of PAN (75 mg/kg). On days 1, 2, 3, and 5 following injection, 24-hour urine collections were obtained for creatinine clearance, albuminuria, and total proteinuria. Then kidneys from each group were fixed by perfusion. Podocytic cytoskeleton was visualized by scanning electron microscopy. Subepithelial GBM staining and attachment fiber number, observed on digitized images of transmission electron micrographs, were quantitated with computer-based density analysis. A significant reduction in attachment fiber number in the GBM lamina rara externa occurred by day 5. On scanning electron micrographs, the secondary and tertiary podocytic processes were observed to be formed by highly aggregated cytoskeleton, which became partially disaggregated by day 3, was totally absent by day 5, and normalized by day 20. Immunogold staining revealed that actin and vinculin localized to the tertiary podocytic processes in the normal state were dispersed into the cell body following PAN. Podocyte cytoskeletal disaggregation precedes, and detachment from the GBM occurs simultaneously with, the onset of massive proteinuria in the PAN model. (Am J Pathol 1993, 142:1641–1653)

Glomerular podocyte dysfunction in disease states leads to remarkable changes in capillary permselectivity and subsequent proteinuria. Normal glomerular visceral epithelial structure, i.e., tertiary foot process and slit diaphragm configuration, is dramatically altered in human minimal lesion disease,[1] primary focal segmental glomerulosclerosis,[2] and membranous glomerulonephritis.[3] Typical changes include loss of tertiary and secondary foot processes, cytosolic vacuolization, loss of normal slit-diaphragm integrity and orientation, and detachment from the glomerular basement membrane (GBM).[4,5]

In the rat models of glomerular epithelial cell toxicity, i.e., puromycin aminonucleoside (PAN) and adriamycin, the same structural and functional abnormalities are observed. We[6] and others[7,8] have demonstrated a close correlation between the onset of massive proteinuria in these models and the detachment of the glomerular epithelium from the GBM. Ryan and Karnovsky,[9] using peroxidase-labeled albumin, have shown that the site of epithelial detachment allows the free passage of macromolecules from the capillary lumen into Bowman's space. However, the biochemical specificity of glomerular podocyte attachment to the GBM and its relationship to other cell functions, e.g., cytoskeletal polymerization, remain only incompletely understood.

It has been speculated that a series of interacting molecules attach the visceral epithelial cytoskeleton through the plasma membrane onto specific receptor sites in the lamina rara externa (LRE) of the GBM.[10] The role of extracellular matrix attachment of many types of epithelium has been well characterized. Mouse mammary epithelial cells bind to fibronectin through a cell-surface proteoglycan.[11] Cultured human amniotic cells and human respiratory epithelial

Supported by a Medical Research Council of Canada grant to the Membrane Biology Group. C. Whiteside is the recipient of an Ontario Ministry of Health Career Development Award.

Accepted for publication October 23, 1992.

Address reprint requests to Dr. C.I. Whiteside, Room 7258, Medical Sciences Building, University of Toronto, 1 King's College Circle, Toronto, Ontario, Canada M5S 1A8.

cells are both able to attach to the proteins of denuded basement membrane *in vitro*.[12] Because the glomerular visceral epithelial cells are continually synthesizing or secreting extracellular matrix protein,[13] it is reasonable to assume that synthesis of both the GBM receptor and the plasma membrane ligand is controlled by this cell. It has been postulated that the anchoring of epithelial cell cytoskeleton to the extracellular matrix, through plasma membrane receptors, stabilizes cell shape, inducing or maintaining a specific differentiative pathway.[14] In this proposed mechanism, detachment of the cells from the matrix, either by loss of specific matrix proteins and/or plasma membrane receptors would lead to a change in cell shape.[15] The toxic cellular changes observed in PAN nephrosis and glomerular epithelial disease states may reflect an acute alteration in new synthesis of extracellular matrix protein.[16,17] However, changes in cytoskeletal aggregation, cell-to-cell attachment, and attachment to the GBM may also reflect PAN-induced changes in the regulation of these specific functions.

To explore further the relationship between glomerular epithelial structure and function, we have used the PAN rat model of nephrosis, focusing on the early sequence of changes in intracellular cytoskeletal aggregation and extracellular GBM attachment. We have adapted a new scanning electron microscopy (SEM) method[18] for the analysis of cytoskeletal structure in glomerular visceral epithelium fixed by perfusion *in vivo*. Immunogold staining was used to localize actin and vinculin in the normal tertiary podocytic processes and the dispersement of these cytoskeletal structural elements following PAN. The *in vivo* fixation method first described by Sakai and Kriz[19] for transmission electron microscopy (TEM) was utilized as well to identify the fibrillar structures in the LRE that join the glomerular epithelium to the GBM. Following PAN administration, decrease in the staining density and number of LRE fibers was observed using a computer-based densitometry analysis of digitized TEM images. Correlations between the onset of proteinuria and specific changes in cytoskeletal aggregation and GBM attachment were examined.

Materials and Methods

PAN Nephrosis

Adult male Sprague-Dawley rats, 400 g, received a single tail-vein injection of puromycin aminonucleoside (ICN Biomedicals Inc., Mississauga, Canada) 75 mg/kg in normal saline. The experimental groups (n = 4/group) consisted of control (no injection), 1, 2, 3, and 5 days postinjection. One day before sacrifice, all four rats in each group had a 24-hour urine collection for creatinine clearance, total protein, and albumin excretion rates. At the time of sacrifice, a 1-ml arterial blood sample was obtained for serum creatinine. The serum and urine creatinine were measured with a standard autoanalyzer method, and creatinine clearance was calculated as:

$$\frac{U \times V}{P}$$

where U is the urine creatinine concentration, V is the urine flow rate, and P is the plasma creatinine concentration. The total urine protein was determined using the Bio-Rad assay (BIO-RAD Chemical Division, Richmond, CA). Urine albumin concentration was measured using a standardized radioimmunoassay with antibody specific for rat albumin.[20] At the time of sacrifice, kidneys were harvested for TEM from three rats and for SEM from one rat in each group (see below).

Preparation of Glomerular Cell Epithelial Cytoskeleton for SEM

Kidneys were cannulated and perfused *in situ*, first with Hanks' buffered salt solution at 37 C followed by the cross-linker 3,3′dithio*bis*(succinimidylpropionate) (Sigma Chemical Co., St. Louis, MO) in Hanks' buffered salt solution for 15 minutes at 37 C, 0.2% Triton X-100 in stabilizing buffer[18] for 15 minutes at 4 C, and finally 1.0% glutaraldehyde in stabilizing buffer for 5 minutes at 4 C. Cortical slices (1 × 1 × 3 mm) were removed and immersed in 1.0% glutaraldehyde in 0.1 mol/L sodium cacodylate buffer (pH 7.4) for 1 hour. After a brief rinse in cacodylate buffer, specimens were immersed in 25% and 50% dimethylsulfoxide for 30 minutes each, snap-frozen in freon, and fractured under liquid nitrogen. The frozen specimens were allowed to thaw in 50% dimethylsulfoxide for 30 minutes and rinsed in distilled water. Conductive staining was performed as follows: 0.5% OsO_4 (aqueous) for 5 minutes, 0.2% tannic acid (aqueous) for 20 minutes at 4 C, and a repeat of the OsO_4 step. Specimens were then dehydrated in a graded ethanol series and critical-point-dried. After identifying the fractured surface, specimens were mounted on stubs, gold-sputtered for 30 seconds, and examined using SEM (Hitachi S-570).

Immunogold Staining of Podocyte Actin and Vinculin

Rat kidney cortex pieces were fixed in 3.0% paraformaldehyde-lysine-periodate solution[21] for 2

hours at 4 C followed by methanol dehydration and embedding in Lowicryl K4M at −20 C.[22] Thin sections were cut, mounted on formvar-coated nickel grids, and processed for immunocytochemistry.

Antibodies used were monoclonal anti-actin (691001 ICN Biomed, Inc., Costa Mesa, CA), monoclonal anti-vinculin (V-9131 Sigma), polyclonal rabbit anti-mouse (Jackson Immunoresearch, Philadelphia, PA), and polyclonal goat anti-rabbit (GAR, Jackson Immunoresearch). Gold particles were prepared by reduction of chloroauric acid ($HAuCl_4$),[23] and GAR was conjugated to the gold particles.[24] For the immunolabeling with monoclonal antibodies, sections were incubated first in the primary antibody for 2 hours, followed by rabbit anti-mouse for 30 minutes and, finally, GAR conjugated to 15-nm gold particles for 30 minutes. Before each antibody incubation, sections were incubated for 5 minutes in 1.0% skim milk in 0.01 mol/L phosphate-buffered saline with 0.02% polyethyleneglycol 6000 and 0.02% Tween 80 (PBS-A) and were washed between incubations with PBS-A, with a final rinse in distilled water. Antibodies were diluted in PBS-A. Incubation of the sections with GAR/gold alone was performed as a control experiment. All incubations and rinses were performed at room temperature. Sections were counterstained with uranyl acetate and examined using an Hitachi H-7000 transmission electron microscope.

Preparation of Glomerulus for Fibrillar Structural Analysis by TEM

Kidneys were perfused with PBS, pH 7.4, at 37 C, followed by a fixative containing 3.0% glutaraldehyde in 0.1 mol/L sodium cacodylate buffer, pH 7.4, with 0.08% $CaCl_2$, 0.5 g/L picric acid and 15 g/L hydroxyethylcellulose. The tissue was cut into small pieces (0.5 mm^3) and immersed in the same fixative overnight. After a 30-minute rinse in sodium cacodylate buffer, specimens were immersed in 5.0% dimethylsulfoxide in 0.1 mol/L maleate buffer for 15 minutes, followed by 1.0% tannic acid in maleate buffer for 3 hours at room temperature in the dark. Specimens were then rinsed in maleate buffer (several changes) for 2 hours and stained in 1.0% uranyl acetate in maleate buffer for 2 hours at 4 C.[25] Then, samples were dehydrated in a graded acetone series at low temperature (30% at 4 C, 50% at 0 C; 70, 90, and 100% at −20 C) for 30 minutes each and infiltrated with epon araldite (Marivac Ltd., Halifax, NS, Canada), starting at −20 C (1:1 epon araldite:acetone for 30 minutes) and gradually warmed to 4 C (3:1 for 30 minutes). Specimens were further infiltrated with 100% epon araldite overnight at room temperature, with several changes of fresh resin, before embedding and polymerization at 65 C for 48 hours. Thin sections were stained with uranyl acetate and lead citrate and examined using TEM (Hitachi H-7000).

Computer-Based Densitometry Analysis of Epithelial Fibrillar Attachment to the GBM

Following random sectioning of the outer kidney cortex and preparation for TEM, three outer cortical glomeruli were chosen randomly from the kidney of each rat. From each glomerulus, three capillary segments were chosen randomly, photographed at ×50,000 and enlarged to an 8 inch × 10 inch print, with a final magnification of ×150,000. The photographic images were digitized with an Hitachi KP-113 video camera and a 386 SX personal computer. One pixel represented 1.1×10^{-5} μm^2 of the digitized image. JAVA software (Jandel Scientific, Corte Madera, CA) was used for gray-scale calibration of each photograph, the lightest pixel representing a gray-scale value of 255 and the darkest pixel representing a gray-scale value of 0. (This allowed the full gray-scale to be utilized and comparison to be made between photographs, normalizing for variable photographic developing intensities.) Next, straight lengths (between 40 to 370 pixels) along the LRE immediately adjacent to the glomerular epithelial tertiary foot processes (excluding the region adjacent to slit diaphragms or epithelial cell–coated pits) were chosen. The corresponding straight lengths along the lamina densa (LD) were measured. The staining density along those lengths was analyzed and the mean ± SD gray-scale value, for the linear regions of interest in the LRE and corresponding LD, was calculated for each photograph. The absolute difference between the mean LRE and LD gray-scale intensity and the ratio LRE/LD was compared between each experimental and control group using the student *t*-test analysis. Variability among rats in each group was also examined.

The pixels ($n = 50$) densitized along each linear segment of the LRE were plotted versus GBM length (300 pixels/μm GBM) Along each length, pixel density troughs below the statistical gray-scale mean were identified as a possible attachment site between the epithelial foot process and the GBM. A drop in the gray-scale value of greater than 5 pixel points, with a subsequent rise of at least 5 pixel points, was considered as a fibrillar structure in the LRE. The number of troughs (assumed fibrillar attachment sites) per μm length of

LRE was calculated. The mean value for each experimental group was then compared to the control value.

Results

PAN Nephrosis—Proteinuria/Albuminuria Profile

As shown in Table 1, within 48 hours post-PAN injection, the 24-hour urine albumin increased significantly. Both total proteinuria and albuminuria suddenly increased between days 3 and 5 and were sustained until day 10, as previously reported.[6] Following PAN injection, there were no sustained changes in creatinine clearance.

Glomerular Visceral Epithelial Cytoskeleton Visualized by SEM

As seen in Figure 1A, the cytoskeletal structure of the visceral epithelial cell occupies the entire cytosolic space. The tertiary foot processes, which are created by the highly aggregated cytoskeleton, extend between the cell body and the GBM (Figure 1B). A higher magnification of cytoskeletal fibers located in the glomerular epithelial cell body reveals a predominance of two fiber sizes, as illustrated in Figure 1B inset. The larger type (a) fibers are 31.0 ± 2.3 nm (mean ± SD, $n = 10$) in width, and the intermediate type (b) fibers are 18.1 ± 0.1 nm ($n = 11$). The smaller cross-linking elements were not analyzed.

Following PAN injection, as illustrated in Figures 2 and 3, the density of the aggregated cytoskeletal structure forming the tertiary foot processes is lost progressively and accompanies flattening or effacement of the epithelium (see TEM below). In Figure 2, A and B, the fibrillar structure of the cell body cytoskeleton appears more loosely knit. By day 5, large cavities, presumably the sites of vacuolization, become apparent (see Figure 3, A and B). By day 20, the cytoskeletal organization returns to almost normal appearance (see Figure 4, A and B).

This method also allowed the visualization of the glomerular endothelial cytoskeletal array. The fenestral openings through the cells created by this structure are still present on day 3 (see Figure 2B). By day 5 following PAN, this array appears altered, with loss of the regular fenestral pattern (see Figure 3B), which returns to a normal appearance by day 20 (see Figure 4A).

Table 1. *PAN Nephrosis — Proteinuria/Albuminuria ($\bar{x}$ ± SD, n = 4 rats/group)*

Days after PAN injection	24-Hour creatine clearance (ml/min)	Total proteinuria (mg/day)	Total albuminuria (μg/day)
Controls	1.56 ± 0.18	53 ± 15	173 ± 85
1 day	2.13 ± 0.50	57 ± 8	265 ± 60
2 days	2.54 ± 1.80	75 ± 19	347 ± 155*
3 days	1.95 ± 0.34	192 ± 14*	458 ± 113*
5 days	3.13 ± 0.22	440 ± 75*	847 ± 177*

* $P < 0.05$ versus control.

Glomerular Visceral Epithelial Cytoskeleton and Attachment to GBM Visualized by TEM

The fibrillar attachment between the visceral epithelium and the GBM in the LRE, as typically visualized by TEM, is shown in Figure 5. Less intense staining of the LRE was observed contiguous to the slit diaphragms. By day 5 following PAN, loss of the tertiary foot processes is associated with decreased overall staining in the GBM (see Figure 6). Although most of the slit diaphragms have disappeared, they are occasionally visualized in sites distant from the GBM (see Figure 6).

Immunogold Staining of Visceral Epithelial Actin and Vinculin

Figure 7A illustrates the immunogold-labeled distribution of actin localized in the tertiary foot processes of the normal rat visceral epithelium, with no staining in the cell body. The control (not shown) experiments without anti-actin antibody revealed no staining of identically prepared glomerular tissue. The only other areas of immunogold staining (not shown) included glomerular mesangial cells and arteriolar smooth-muscle cells. Figure 7B reveals the distribution of immunogold-stained actin 5 days post-PAN injection. Actin is now distributed uniformly throughout the epithelial cell body.

Figure 8A reveals immunogold-labeled vinculin principally at the tertiary foot process–GBM interface in the normal rat podocyte. However, 5 days post-PAN, vinculin is found distant from the GBM interface in the cell body cytosol. The control experiments (not shown), in the absence of the anti-vinculin antibody, demonstrated no staining of identically prepared glomerular tissue.

Computer-Based Densitometry Analysis of Epithelial Attachment

Figure 9 illustrates the typical TEM samples used for the computer-based densitometry analysis of the

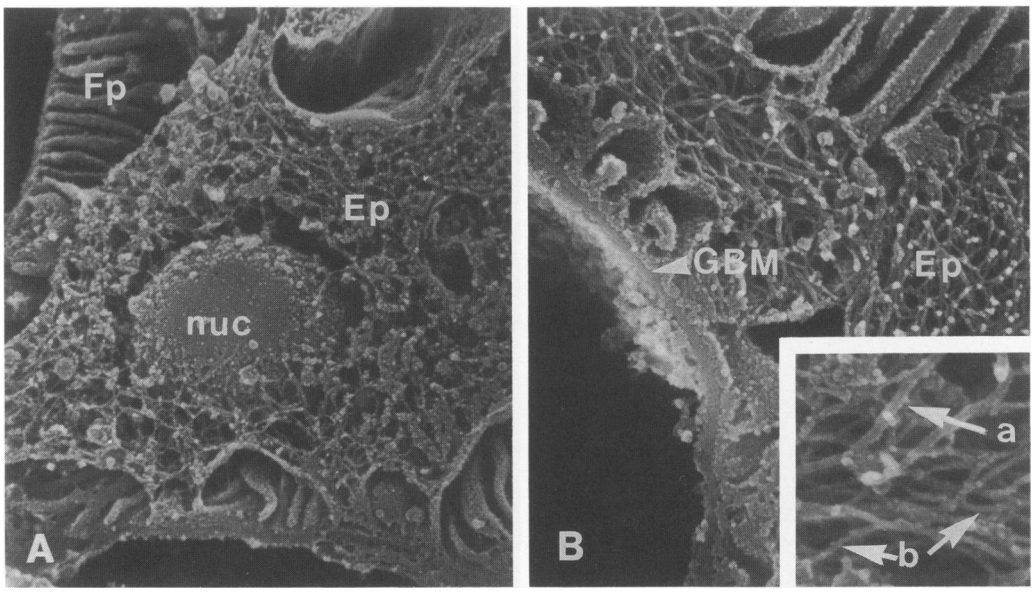

Figure 1. A: *Scanning electron micrograph of a normal rat glomerular visceral epithelial cell (Ep) showing the cytoskeletal network surrounding the nucleus (nuc). The tertiary foot processes (Fp) are composed of densely aggregated cytoskeleton (×13,000).* B: *The alignment of normal tertiary foot processes on the glomerular basement membrane (GBM) is shown (×26,000). Inset: Cytoskeleton of the cell body (×52,000) with a predominance of large type a fibers and intermediate-sized type b fibers.*

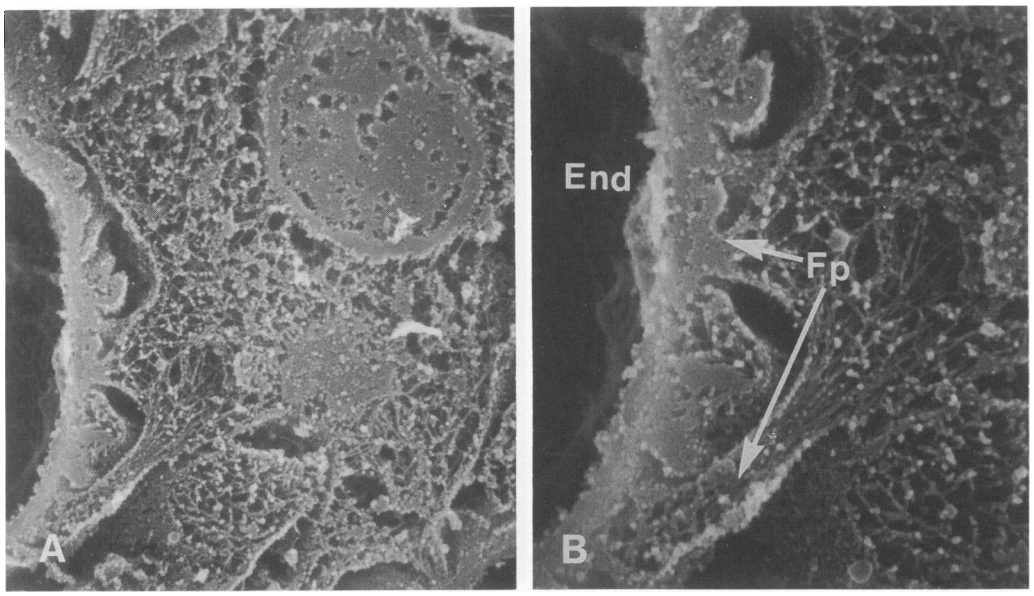

Figure 2. A: *Scanning electron micrograph of rat glomerular visceral epithelial cell 3 days following PAN injection (×13,000).* B: *There is partial loss of foot process (Fp) definition. The cytoskeleton of the endothelium (End), creating the fenestrae, is intact (×26,000).*

LRE and LD staining intensity. In the control sample (Figure 9A), the arrows point to the subepithelial areas of interest in the LRE. Through day 1 (Figure 9B), day 3 (Figure 9C), and day 5 (Figure 9D), there is a progressive loss of staining in the LRE as well as in the LD. It is noted that on days 1 and 3 simple visualization does not distinguish subtle changes in density in the LRE and LD that are apparent with computer-based densitometry analysis. Specifically, the absolute density and relative density to the LD within the LRE decreased as the tertiary foot process structure disappeared. In Table 2, following PAN injection, the gray-scale intensities (mean ± SD, n = 30 to 40/group) along the LRE and the corresponding LD of the GBM are shown. By day 1 in the LRE and by day 2 in the LD, there is a significant change in density compared to that observed in control samples. There is a small but significant change in the difference between the LRE and LD by day 1, but no significant change from days 1 to 5 in the LRE/LD values. No consistent or significant differences were observed in the mean LRE or LD

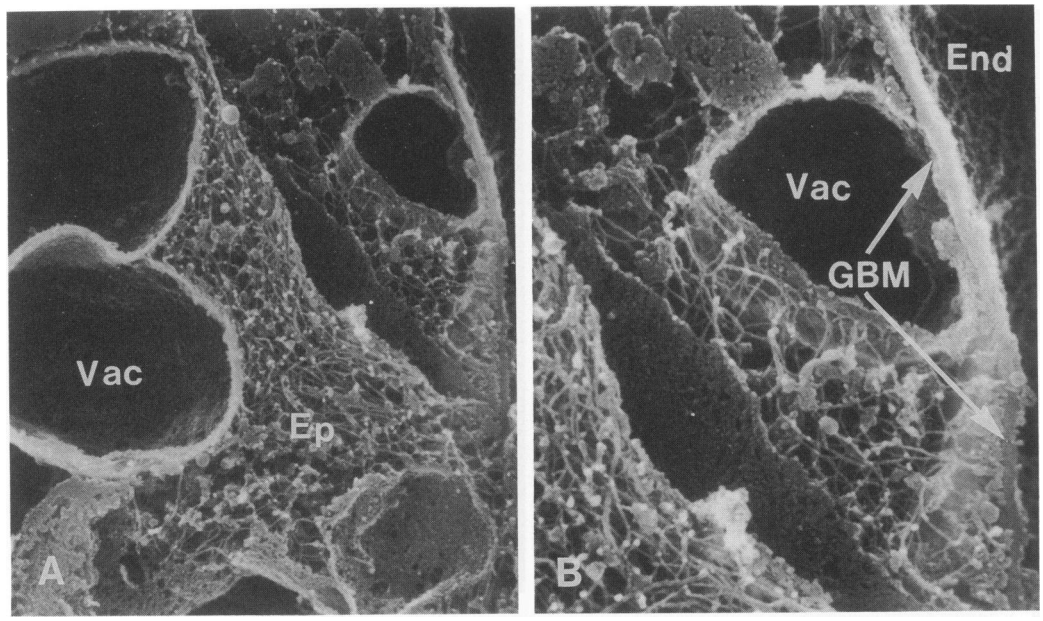

Figure 3. A: *Scanning electron micrograph of rat visceral epithelial cell (Ep) 5 days post-PAN injection. Vacuoles (Vac) have now appeared in the cell body (×13,000).* B: *The tertiary foot processes have disappeared along the GBM. The cytoskeletal endothelium (End) no longer has the regular fenestrated pattern (×26,000).*

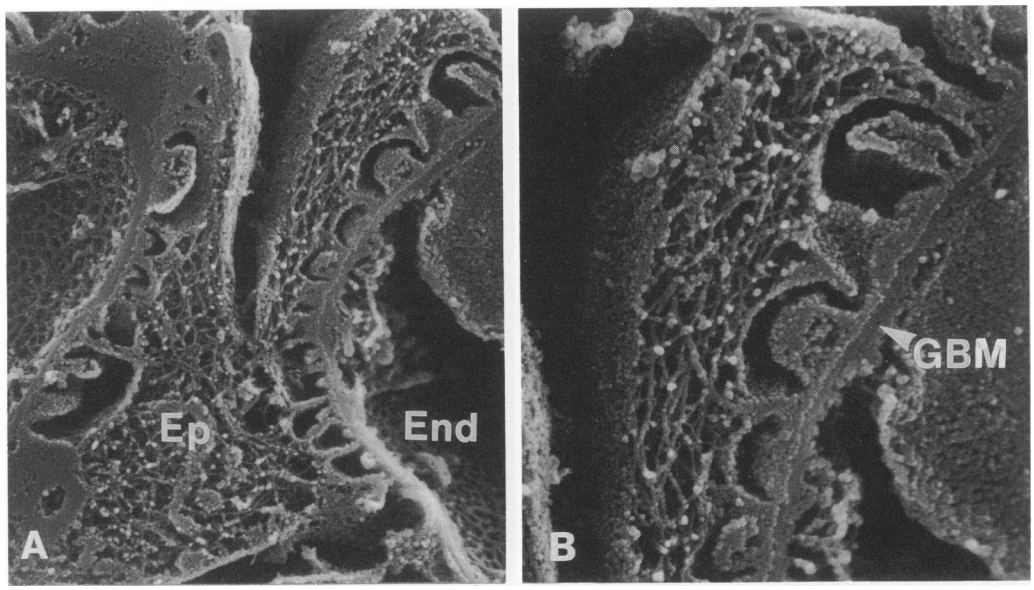

Figure 4. A: *Scanning electron micrograph of rat visceral epithelial cell (Ep) 20 days post-PAN injection. The endothelial (End) cytoskeletal fenestrated pattern has returned (×13,000).* B: *Restoration of tertiary foot processes along the GBM is shown (×26,000).*

gray-scale intensity values among the 3 rats in each experimental group (data not shown).

Figure 10 illustrates the change in gray-scale intensity along the typical 1-μm length of GBM from control (upper panel) and day 5 (lower panel) sample. By day 5, the pattern is simplified, consistent with a decreased number of attachment sites. As shown in Table 3, the decreased attachment site density in the LRE does not reach statistical significance until day 5.

Discussion

In human glomerulonephritis associated with nephrotic syndrome, the highly differentiated state of the podocyte processes is absent. However, the connection between loss of tertiary foot processes and the cause of massive proteinuria remained enigmatic until detailed studies in the PAN rat model were performed to identify a cause-and-effect relationship between altered podocyte structure and function. A correlation between the sudden

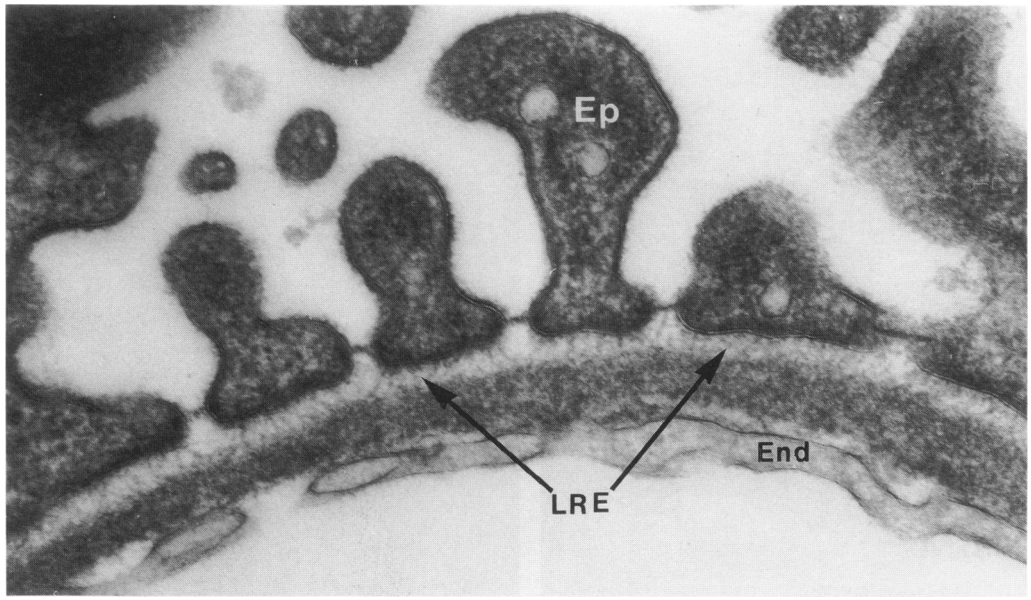

Figure 5. *Transmission electron micrograph of a normal rat glomerular capillary wall. The fixation enhances the view of fibrillar attachment of the glomerular visceral epithelium (Ep) to the basement membrane through the LRE—see arrows. The normally fenestrated endothelial cytoskeleton (End) is shown (×87,000).*

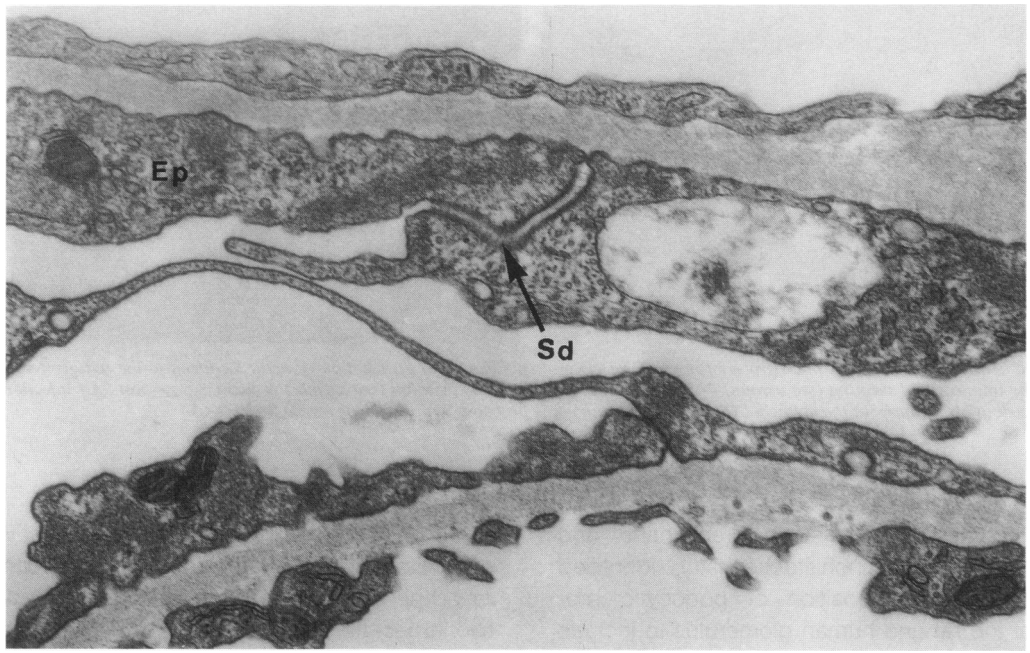

Figure 6. *Transmission electron micrograph of the glomerular capillary walls of the rat 5 days post-PAN injection. There is a loss of tertiary foot processes in the glomerular epithelium (Ep). The normal slit diaphragm (Sd) structure has been disrupted and is displaced above the GBM (×35,000).*

onset of massive proteinuria and the appearance of glomerular podocyte detachment from the GBM has been reported by Messina et al[7] and ourselves[6] in PAN nephrosis. In the present study, we have identified further a temporal relationship between changes in glomerular visceral epithelial cell cytoskeletal aggregation and decreased fibrillar attachment of the epithelium to the GBM with the onset of massive proteinuria.

For the first time, an *in vivo* preparation of perfusion-fixed glomerular tissue has been used to visualize the cytoskeleton of the visceral epithelial cell. In the normal rat, it is apparent that the secondary and tertiary foot processes are formed by

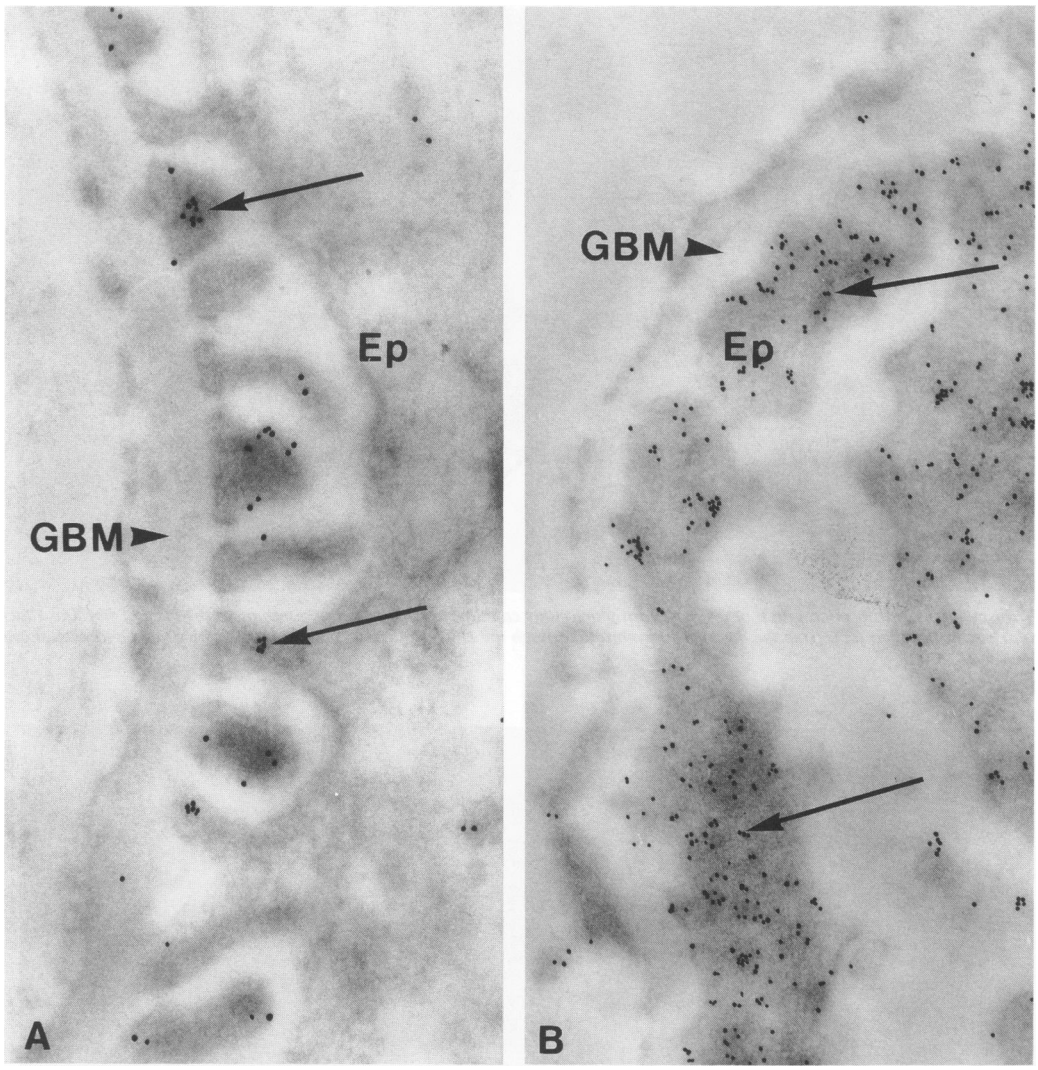

Figure 7. A: *Transmission electron micrograph of normal rat visceral epithelial (Ep) distribution of actin localized to the tertiary foot processes, visualized by immunogold staining (see arrows) (×52,000).* B: *Immunogold localization (see arrows) of actin 5 days post-PAN injection shows a uniform distribution throughout the epithelial (Ep) cytosol. Tertiary foot processes are no longer visible (×39,000).*

densely packed cytoskeleton. Drenckhahn and Franke,[10] using immunohistochemistry, identified the cytoskeletal composition of podocytic processes of the rat and human glomerulus to include actin, myosin, and α-actinin. In the chicken kidney, the same authors identified the presence of vinculin and talin in the plasmalemmal portion of the foot processes that abut the GBM. Using immunogold, we have localized actin to the tertiary foot processes and vinculin to the GBM interface in normal rat podocytes. Actin is a major component of the densely packed cytoskeleton that maintains the tertiary foot process structure, as demonstrated on SEM (see Figure 1, A and B). Vinculin is likely an important component of the GBM attachment complex.

Our SEM studies indicate that the normal visceral epithelial cell body is filled with a more loosely arrayed network of larger fibers. Measurement of the two largest fibers is in keeping with the presence of microtubules and microfilaments. In adult Sprague-Dawley rat glomerular epithelium, Vasmant et al[26] measured microtubules to be 25 nm and microfilaments to be 10 nm in diameter. Because the SEM method requires some gold-sputtered covering of the cytoskeletal structures, our measurement of mean diameters, 31.0 nm and 18.1 nm, may be an overestimate of true microtubular and microfilament diameters.

The combination of immunogold staining visualized by TEM and our new cytoskeletal SEM method identified a clear correlation between loss of foot

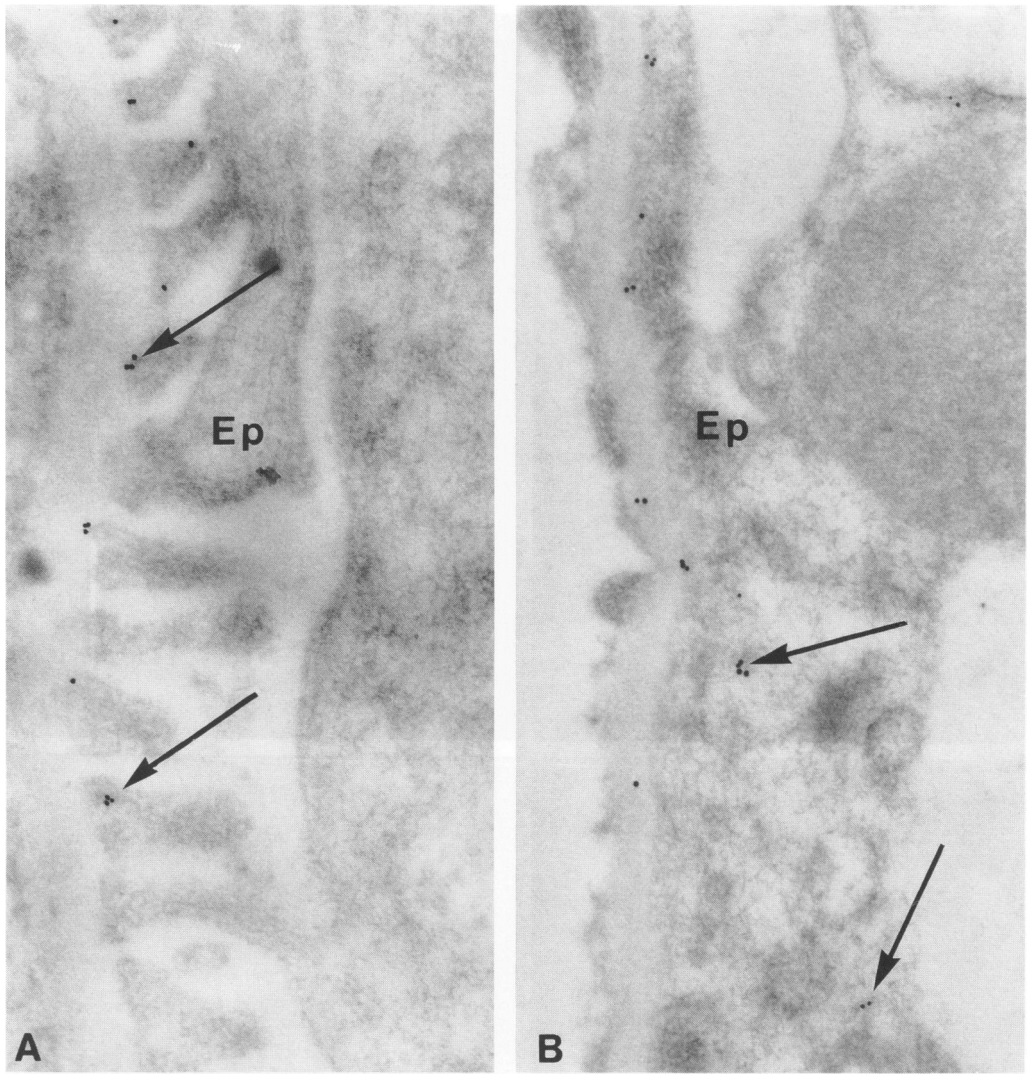

Figure 8. A: *Transmission electron micrograph of normal rat visceral epithelial (Ep) distribution of vinculin localized (see arrow) by immunogold staining primarily to the podocyte-GBM interface (×52,000).* B: *Immunogold localization (see arrows) of vinculin 5 days post-PAN injection reveals a less uniform distribution, now including the epithelial (Ep) cytosol (×520,000).*

process cytoskeletal actin aggregation and the onset of massive proteinuria 3 to 5 days following PAN injection. A similar finding has been reported recently by Lachapelle and Bendayan.[27] The enhanced immunogold staining of actin in the visceral epithelial cell body 5 days following PAN (see Figure 7B) may be a result of more available epitopesites on disaggregated (globular) actin. Following PAN, the cytoskeleton that fills the normal glomerular epithelial cell body becomes cavitated, presumably due to the formation of vacuoles. Previously, Messina et al[7] have postulated that the contiguous array of vacuoles across the glomerular epithelium between the GBM and Bowman's space may permit the hydrostatic pressure to blow out the weakened epithelial cell. This may be one site of the functional protein shunts in human glomerular disease characterized by nephrotic-range proteinuria described by Deen et al[28,29] and by ourselves[30] in the PAN and adriamycin rat models. Bohrer et al[31] first reported the results of neutral and anionic dextran fractional clearances in PAN rats, suggesting that the glomerular wall develops a charge-selective defect. Based on further studies using larger-sized dextrans, it has been shown that the increased permeability of these dextrans (>50 Å Stokes-Einstein radius) can be explained only by the appearance of effective large shunts across the capillary wall.

The defect in rat glomerular permeability within the first 3 days following PAN injection, allowing increased albuminuria (non-nephrotic proteinuria), could be explained by a decrease in polyanionic charge. Mahan et al[32] have reported a similar early onset of albuminuria within 48 hours of PAN injection. Previously, we have documented a significant decrease in heparan sulfate content of isolated glo-

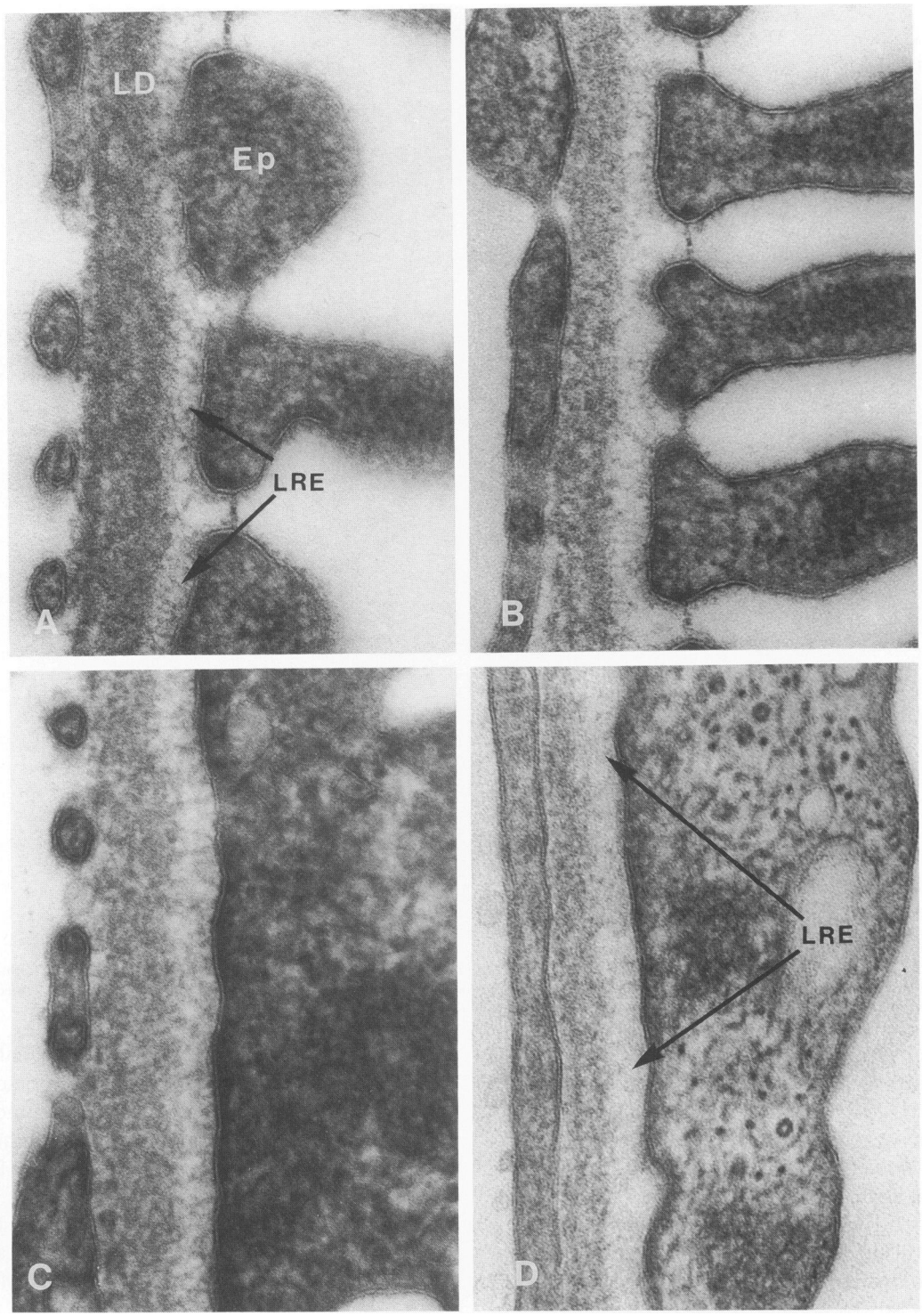

Figure 9. A: *Transmission electron micrograph of normal rat glomerular epithelial (Ep) cells attached to the glomerular basement membrane. Attachment fibers are shown in the LRE—see arrows. Enhanced staining of the LD is also shown (×130,000).* B: *One day following PAN injection, there is decreased density in the LRE and LD. The slit diaphragms and tertiary foot processes are intact (×130,000).* C: *Three days following PAN injection, there is a loss of tertiary foot processes and slit diaphragms (×130,000).* D: *Day 5 post-PAN injection. There is a significantly reduced number of fibrillar attachments between the glomerular epithelium and basement membrane in the LRE—see arrows (×130,000).*

meruli and reduced polyethyleneimine staining of the LRE of the rat GBM within 48 hours following PAN injection.[6] In the current study, a decline in GBM staining was observed first in the LRE (by day 1 post-PAN) and then in the LD (by day 2), perhaps related to reduced heparan sulfate content. Liu et al[33] have reported that PAN inhibits murine metanephric proteoglycan synthesis, which prevents dif-

Table 2. *Pixel Gray-Scale Intensities*

Days after PAN (3 rats/group)	Gray-scale intensity			
	LRE	LD	LRE-LD	LRE/LD
Control	103±30	65±30	39±18	1.76±.52
1 day	129±31*	77±21†	52±19*	1.82±.47†
2 days	143±41*	84±30*	58±22*	1.86±.54†
3 days	153±35*	101±32*	53±17*	1.62±.34†
5 days	141±36*	95±32*	46±15†	1.54±.22†

White = 255, black = 0 ($\bar{x}$ ± SD, n = 27 photos/group) along the *lamina rara externa* (LRE) and the corresponding *lamina densa* (LD) of the glomerular basement membrane following PAN injection.

* $P < 0.05$ versus control.

† NS versus control.

Table 3. *Effect of PAN on Fiber Density in the LRE of the Glomerular Basement Membrane*

Days after PAN (3 rats/group)	Number of density troughs (fibers) per μm GBM ($\bar{x}$ ± SD)
Control	16.9 ± 0.6 (n* = 32)
1 day	16.7 ± 1.8† (n = 29)
2 days	15.5 ± 0.5† (n = 31)
3 days	14.5 ± 1.7† (n = 35)
5 days	10.3 ± 1.4‡ (n = 36)

* No. of μm GBM lengths measured (10 to 12 μm/rat).

† NS versus control.

‡ $P < 0.01$ versus control.

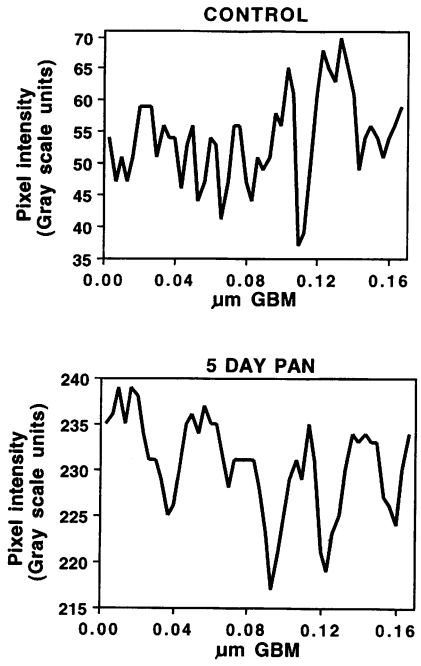

Figure 10. Upper panel: *gray-scale intensity pattern along the LRE observed in normal control rat GBM.* Lower panel: *5 days following PAN injection, fiber density is indicated by a significant reduction in the number of troughs (300 pixels/μm GBM length).*

ferentiation of the visceral epithelial foot processes. Loss of tertiary foot processes in PAN nephrosis and human glomerulonephritis may represent a dedifferentiated state of the podocytes associated with decreased heparan sulfate synthesis.

The subepithelial fibrillar attachment pattern along the LRE remained intact until day 5 following PAN injection, despite the reduced staining density in both LRE and LD. Further evidence that the epithelial attachment complex is no longer intact by day 5 post-PAN is provided by the immunogold localization of vinculin, which is no longer at the GBM interface. Combining the SEM and TEM data in the PAN model, loss of tertiary foot process cytoskeletal aggregation seems to begin by day 3, preceding the significant reduction in fibrillar attachment density between the epithelium and GBM. Albuminuria continually increased between days 2 and 5 post-PAN injection, although massive proteinuria was observed only by day 5. It is likely that a critical degree of cytoskeletal disaggregation and attachment complex disruption must evolve before podocyte detachment[6] and massive proteinuria are observed in this model.

The effect of PAN on glomerular visceral epithelial cells is reminiscent of those seen in the renal tubular epithelium *in vivo* and *in vitro* following hypoxic injury.[34] The polarity and differentiation of tubular cells are maintained by cell-to-cell contact and attachment to the extracellular matrix.[35,36] During injury that results in loss of tight-junction integrity, the tubular cells lose their polarity and in turn attachment to the extracellular matrix. The organization of the intracellular cytoskeletal array also disappears. Injury leads to a dedifferentiation process[37] similar to that observed in PAN-induced glomerular toxicity. Avasthi and Evan[38] have reported the loss of glomerular endothelial fenestrae following PAN treatment. Our SEM data suggest that loss of endothelial cytoskeletal organization may play a role in this process.

These findings in the PAN model suggest that mediators of human glomerular disease that cause podocyte dysfunction may operate through specific cellular mechanisms involving the regulation of cytoskeleton and attachment to the GBM. These may include cellular signaling pathways that control cytoskeletal polymerization, synthesis of GBM attachment proteins, or both.

Acknowledgments

We are grateful to Madeleine C. Miller for excellent secretarial assistance.

References

1. Chiang ML, Hawkins EP, Berry PL, Barrish J, Hill LL: Diagnostic and prognostic significance of glomerular epithelial cell vacuolization and podocyte effacement in children with minimal lesion nephrotic syndrome

and focal segmental glomerulosclerosis: an ultrastructural study. Clin Nephrol 1988, 30:8–14
2. Verani RR, Hawkins EP: Recurrent focal segmental glomerulosclerosis, a pathological study of the early lesion. Am J Nephrol 1986, 6:263–270
3. Okada K, Kawakam K, Miyao M, Oite T: Ultrastructural alterations of glomerular anionic sites in idiopathic membranous glomerulonephritis. Clin Nephrol 1986, 26:7–14
4. Yoshikawa V, Ito H, Akamatsu R, Hazikano H, Okada S, Matsuo T: Glomerular podocyte vacuolization in focal segmental glomerulosclerosis. Arch Pathol Lab Med 1986, 110:394–398
5. Grishman E, Churg J: Glomerular sclerosis in nephrotic patients: an electron microscopic study of glomerular podocytes. Kidney Int 1975, 7:111–122
6. Whiteside C, Prutis K, Cameron R, Thompson J: Glomerular epithelial detachment, not reduced charge density, correlates with proteinuria in adriamycin and puromycin nephrosis. Lab Invest 1989, 61:650–660
7. Messina A, Davies DJ, Dillane PC, Ryan GB: Glomerular epithelial abnormalities associated with the onset of proteinuria in aminonucleoside nephrosis. Am J Pathol 1987, 126:220–229
8. Venkatachalam MA, Cotran RS, Karnovsky MJ: Glomerular studies in experimental nephrosis using horseradish peroxidase as a tracer. J Exp Med 1969, 132:1168–1180
9. Ryan GB, Karnovsky MJ: Ultrastructural study of the mechanisms of proteinuria in aminonucleoside nephrosis. Kidney Int 1975, 3:219–232
10. Drenckhahn D, Franke RP: Ultrastructural organization of contractile and cytoskeletal proteins in glomerular podocytes of chicken, rat and man. Lab Invest 1988, 59:673–682
11. Saunders S, Bernfield M: Cell surface proteoglycan binds mouse mammary epithelial cells to fibronectin and behaves as a receptor for interstitial matrix. J Cell Biol 1988, 106:423–430
12. Vanaille TJ, Mendis AHW, Warton A, Walker L, Papadimitriou JM, Robinson BW: Study of human epithelial cell detachment and damage: development of a model. Immunol Cell Biol 1989, 67:359–369
13. Stow JL, Sawada H, Farquhar MG: Basement membrane heparan sulfate proteoglycans are concentrated in the lamina rarae and in the podocytes of the rat renal glomerulus. Proc Natl Acad Sci USA 1985, 82:3296–3300
14. Rodriguez-Bolilan E, Nelson WJ: Morphogenesis of the polarized epithelial cell phenotype. Science 1989, 245:718–725
15. Rapraeger A, Jalkanen M, Bernfield M: Integral membrane proteoglycans as matrix receptors: role of cytoskeleton and matrix assembly at the epithelial cell surface. Biology of Proteoglycans. Edited by Wight TN, Mecham RP, 1987, Orlando, Academic Press, pp 129–154
16. Kasinath BS, Singh AK, Kanwar YS, Lewis EJ: Effect of puromycin aminonucleoside on HSPG core protein content of glomerular epithelial cells. Am J Physiol 1988, 255:F590–F598
17. Groggel GC, Hovingh P, Border WA, Linker A: Changes in glomerular heparan sulfate in puromycin aminonucleoside nephrosis. Am J Pathol 1987, 128: 521–527
18. Bell PB, Lindroth M, Fredriksson B-A, Liu X-X: Problems associated with the preparation of whole mounts of cytoskeletons for high resolution in electron microscopy. Scanning Microsc Int 1989, (Suppl) 3:117–135
19. Sakai T, Kriz W: The structural relationship between mesangial cells and basement membrane of the renal glomerulus. Anat Embryol 1987, 176:373–386
20. Whiteside CI, Thompson J: The role of angiotensin II in progressive diabetic glomerulopathy in the rat. Endocrinology 1989, 125:1932–1940
21. McLean IW, Nakane PK: Periodate-lysine-paraformaldehyde fixative: a new fixative for electron microscopy. J Histochem Cytochem 1974, 22:1077–1083
22. Bendayan M: Protein A-gold electronmicroscopic immunocytochemistry: methods, applications and limitations. J Electron Microsc Tech 1984, 1:243–270
23. De Mey J: Colloidal gold as a marker and tracer in light and electron microscopy. EMSA Bull 1984, 14: 54–65
24. Geohegan WD: Adsorption of horseradish peroxidase, ovomucoid and anti-immunoglobulin to colloidal gold for the indirect detection of Concanavalin A, wheat germ agglutinin and goat anti-human immunoglobulin G on cell surfaces at the electron microscopic level: a new method, theory and application. J Histochem Cytochem 1977, 25:1187–1200
25. Mbassa G, Elger M, Kriz W: The ultrastructural organization of the basement membrane of Bowman's capsule in the rat renal corpuscle. Cell Tissue Res 1988, 253:151–163
26. Vasmant D, Maurice M, Feldmann G: Cytoskeleton ultrastructure of podocytes and glomerular endothelial cells in man and in the rat. Anat Rec 1984, 210:17–24
27. Lachapelle M, Bendayan M: Contractile proteins in podocytes: immunocytochemical localization of actin and alpha-actinin in normal and nephritic rats. Virchows Archiv [B] 1991, 60:105–111
28. Deen WM, Bridges GR, Brenner BM, Myers BD: Heteroporous model of glomerular size selectivity: application to normal and nephrotic humans. Am J Physiol 1985, 249:F374–F389
29. Tomlanovich S, Deen WM, Jones III HW, Schwartz HC, Myers BD: Functional nature of glomerular injury in progressive diabetic glomerulopathy. Diabetes 1987, 36:556–565
30. Whiteside CI, Lumsden CJ, Zlotnik M: Glomerular epithelial detachment in puromycin and adriamycin nephrosis correlates with anionic dextran leak through shunts (abs) 1989, Workshop on the Biology of the Renal Microvasculature, Renal Physiology/Cell Biology Program, Division of Kidney, Urologic and Hematologic Diseases, NIDDK-NIH

31. Bohrer MP, Baylis C, Robertson CR, Brenner BM: Mechanisms of the puromycin-induced defects in the transglomerular passage of water and macromolecules. J Clin Invest 1977, 60:152–161
32. Mahan JD, Sisson-Ross S, Vernier RL: Glomerular basement membrane anionic charge site changes early in aminonucleoside nephrosis. Am J Pathol 1986, 125:393–401
33. Liu ZZ, Dalecki TM, Kashihara N, Wallner EI, Kanwar YS: Effect of puromycin on metanephric differentiation: morphological, autoradiographic and biochemical studies. Kidney Int 1991, 39:1140–1155
34. Molitoris BA, Hoi Lien CA, Dahl R, Ahnen DJ, Wilson PD, Kim J: Characterization of ischemia-induced loss of epithelial polarity. J Membr Biol 1988, 106: 233–242
35. Molitoris BA, Kinne R: Ischemia induces surface membrane dysfunction. Mechanism of altered Na^+-dependent glucose transport. J Clin Invest 1987, 80: 647–654
36. Nelson WH, Veshnock PJ: Modulation of Fodrin (membrane skeleton) stability by cell-cell contact in Madin-Darby canine kidney epithelial cells. J Cell Biol 1987, 104:1527–1537
37. Bacallao R, Fine LG: Molecular events in the organization of renal tubular epithelium: from nephrogenesis to regeneration. Am J Physiol 1989, 257:F913–F924
38. Avasthi PS, Evan AP: Glomerular permeability in aminonucleoside-induced nephrosis in rats. A proposed role of endothelial cells. J Lab Clin Med 1979, 93:266–276